

# Bifunctionality of the Thiamin Diphosphate Cofactor: Assignment of Tautomeric/Ionization States of the 4'-Aminopyrimidine Ring When Various Intermediates Occupy the Active Sites during the Catalysis of Yeast Pyruvate Decarboxylase

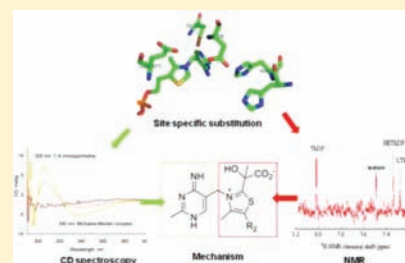
Anand Balakrishnan,<sup>‡</sup> Yuhong Gao,<sup>‡</sup> Prerna Moorjani,<sup>‡</sup> Natalia S. Nemeria,<sup>‡</sup> Kai Tittmann,<sup>†</sup> and Frank Jordan<sup>\*‡</sup>

<sup>†</sup>Albrecht-von-Haller Institute & Göttingen Center for Molecular Biosciences, Georg-August University, Göttingen, D-37077 Göttingen, Germany

<sup>‡</sup>Department of Chemistry, Rutgers University, Newark, New Jersey 07102, United States

**S** Supporting Information

**ABSTRACT:** Thiamin diphosphate (ThDP) dependent enzymes perform crucial C–C bond forming and breaking reactions in sugar and amino acid metabolism and in biosynthetic pathways via a sequence of ThDP-bound covalent intermediates. A member of this superfamily, yeast pyruvate decarboxylase (YPDC) carries out the nonoxidative decarboxylation of pyruvate and is mechanistically a simpler ThDP enzyme. YPDC variants created by substitution at the active center (D28A, E51X, and E477Q) and on the substrate activation pathway (E91D and C221E) display varying activity, suggesting that they stabilize different covalent intermediates. To test the role of both rings of ThDP in YPDC catalysis (the 4'-aminopyrimidine as acid–base, and thiazolium as electrophilic covalent catalyst), we applied a combination of steady state and time-resolved circular dichroism experiments (assessing the state of ionization and tautomerization of enzyme-bound ThDP-related intermediates), and chemical quench of enzymatic reaction mixtures followed by NMR characterization of the ThDP-bound intermediates released from YPDC (assessing occupancy of active centers by these intermediates and rate-limiting steps). Results suggest the following: (1) Pyruvate and analogs induce active site asymmetry in YPDC and variants. (2) The rare 1',4'-iminopyrimidine ThDP tautomer participates in formation of ThDP-bound intermediates. (3) Propionylphosphinate also binds at the regulatory site and its binding is reflected by catalytic events at the active site 20 Å away. (4) YPDC stabilizes an electrostatic model for the 4'-aminopyrimidinium ionization state, an important contribution of the protein to catalysis. The combination of tools used provides time-resolved details about individual events during ThDP catalysis; the methods are transferable to other ThDP superfamily members.



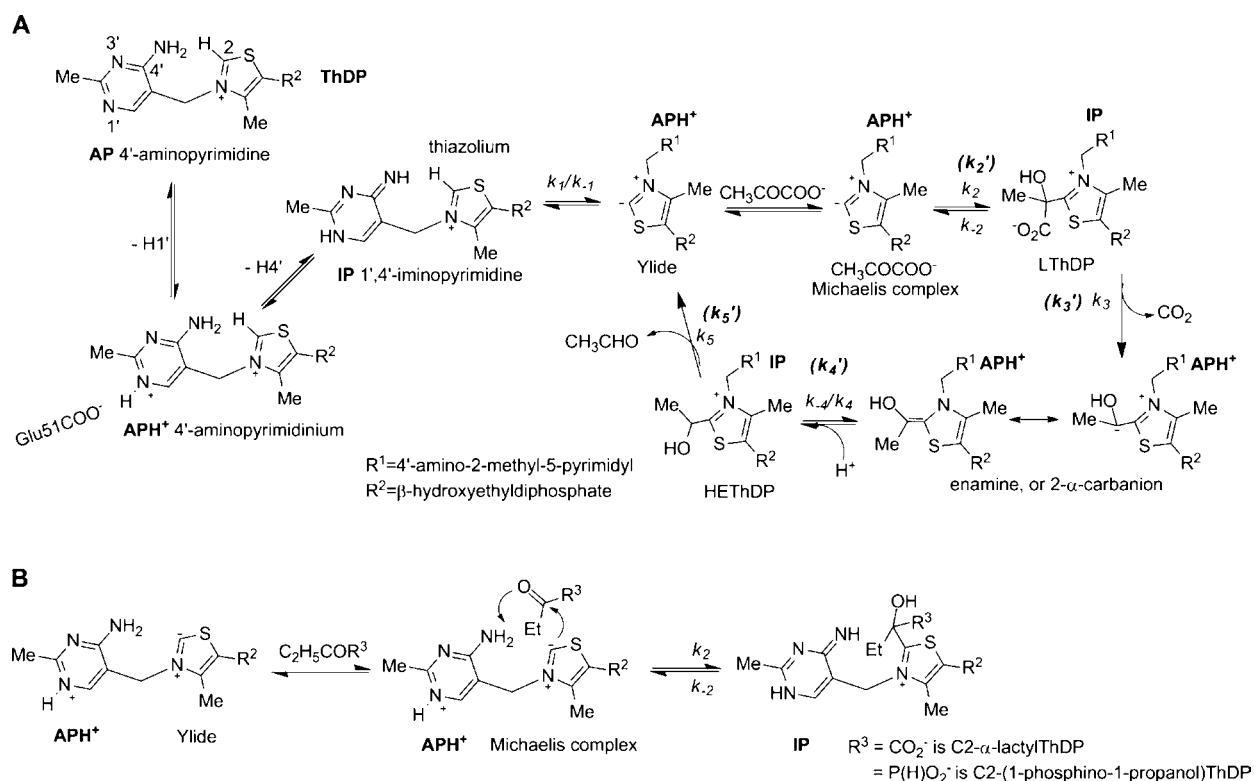
## INTRODUCTION

Yeast pyruvate decarboxylase (YPDC, EC 4.1.1.1), a thiamin diphosphate (ThDP) and  $Mg^{2+}$  dependent enzyme catalyzes the nonoxidative decarboxylation of pyruvate to acetaldehyde. YPDC is an  $\alpha_4$  homotetramer of  $M_r = 250\,000$  and is subject to activation by substrate<sup>1</sup> and by the substrate activator surrogate pyruvamide.<sup>2</sup> The cofactor ThDP is bound at the interface created by two monomers that form a tight dimer. This tight dimer known as the “functional dimer” is the minimal catalytically active unit<sup>3–5</sup> and two of these functional dimers assemble into a loose tetramer in the quaternary structure. X-ray crystallographic studies showed the coenzyme ThDP bound in the “V” conformation in the active sites of YPDC.<sup>6,7</sup> This unusual conformation of the ThDP brings the C2 and N4' atoms within close contact (to less than 3.5 Å) of each other.<sup>8</sup> A consensus of chemical steps based on five decades of research on the YPDC catalyzed decarboxylation of pyruvate is shown in Scheme 1A, and involves a series of covalent ThDP-bound intermediates, including the predecarboxylation C2 $\alpha$ -lac-

tylThDP (LThDP), the enamine resulting from decarboxylation, and the postdecarboxylation C2 $\alpha$ -hydroxyethylThDP (HETHDP) intermediates. The role of the 4'-aminopyrimidine ring in acid–base catalysis and activation of the thiazolium C–H bond has been elucidated<sup>9</sup> aided by circular dichroism spectroscopic (CD) studies, providing evidence for the presence of not only the 4'-aminopyrimidine (AP form) but also of the 1',4'-iminopyrimidine (IP) tautomeric form in YPDC catalysis. These CD studies suggested that in the LThDP and HETHDP intermediates with tetrahedral substitution at C2 $\alpha$ , the 1',4'-iminopyrimidine IP tautomeric form predominates at pH values near and above the  $pK_a$  of the enzyme-bound 4'-aminopyrimidinium (APH<sup>+</sup>) ionization state.<sup>10–15</sup> Concurrently, a complementary method using rapid acid quench of reaction mixtures in combination with <sup>1</sup>H NMR detection was developed; it is capable of

Received: November 28, 2011

Published: February 2, 2012

Scheme 1. (A) Mechanism of Catalytic Cycle of Yeast Pyruvate Decarboxylase and (B) Mechanism of Formation of the 1',4'-iminoPThDP<sup>a</sup>

<sup>a</sup>In bold font are the net forward rate constants for individual steps. The bold abbreviations APH<sup>+</sup>, AP, and IP above each intermediate refer to the predominant ionization/tautomerization state of the 4'-aminopyrimidine in that particular intermediate.

quantification of the relative concentration of covalent ThDP-bound intermediates, and hence the relative rates of individual steps in the mechanism on many ThDP enzymes.<sup>16</sup> While both methods have some limitations (CD methods are limited by lack of direct absorption spectroscopic signatures for pyruvate-derived ThDP-bound covalent intermediates, the chemical quench NMR method does not provide information about the enzyme bound tautomeric form of the 4'-aminopyrimidine ring and cannot differentiate between the enamine and the HEThDP intermediate), a combination of the two methods could provide information about the state of ionization/tautomerization of the 4'-aminopyrimidine ring and about the covalent ThDP-bound intermediates. This powerful combination enables us to gain insight to the catalytic contributions of both the 4'-aminopyrimidine and the thiazolium rings on ThDP enzymes as shown in Scheme 1A.

Two recent studies on ThDP enzymes also suggested that our understanding of the detailed role of the cofactor, of the conserved glutamate at the active centers, and of acid–base catalysis of ThDP enzymes is still incomplete. (1) The enzyme benzaldehyde lyase (BAL; EC 4.1.2.38) carries out reversible decomposition of (*R*)-benzoin to two molecules of benzaldehyde; in the reverse direction the enzyme is a carboligase. The BAL structure contained only two acid–base residues surrounding the ThDP at the active center:<sup>17–19</sup> the highly conserved E50 within hydrogen bonding distance of the N1' atom of the 4'-aminopyrimidine ring, and the H29 residue. The residue H29 is too far from the thiazolium C2 atom to be useful in the first steps of the reaction, and was suggested to have a function in removing the β-hydroxyl proton of the ThDP-

bound benzoin to assist release of the first benzaldehyde molecule. Because of the paucity of potential acid–base residues, the pH dependence of the steady-state kinetic parameters on BAL could be interpreted rather unambiguously: a residue was implicated in either the  $k_{\text{cat}}\text{-pH}$  or  $k_{\text{cat}}/K_{\text{M}}\text{-pH}$  profile with  $pK_{\text{a}} = 5.3$  at the acidic side, likely corresponding to the highly conserved glutamate residue<sup>20</sup> and providing the first  $pK_{\text{a}}$  value for this conserved glutamate. (2) The structure of the enzyme glyoxylate carboligase [(GCL; EC 4.1.1.47) carries out a carboligation reaction after decarboxylation of the first molecule of glyoxylate to the enamine intermediate] revealed even greater surprises. This enzyme is not only devoid of acid–base groups at its active center within hydrogen bonding distance of ThDP, it is also lacking the highly conserved Glu, in its place there is a hydrophobic valine residue.<sup>21</sup>

To further our understanding of the various roles of the highly conserved glutamate and of other acidic amino acid residues implicated in the mechanism, we undertook steady state and transient state studies on YPDC variants produced earlier by substitutions at the catalytically important glutamate and aspartate residues (Figure 1), which are proposed to be involved in essential proton transfer steps.<sup>22,23</sup> Specifically, variants of (i) the highly conserved E51 [believed to catalyze the tautomerization at the N1' position of the cofactor<sup>24</sup>], (ii) D28 and E477 [residues which assist in the protonation of the enamine and acetaldehyde release<sup>3,22,25</sup>], and (iii) C221 and E91 [the former is the locus of allosteric regulation,<sup>26,27</sup> and the latter is situated at the interface of three domains and plays a central role in interdomain communication from the allosteric β domain and C221 to the α domain (H92 the recipient of the

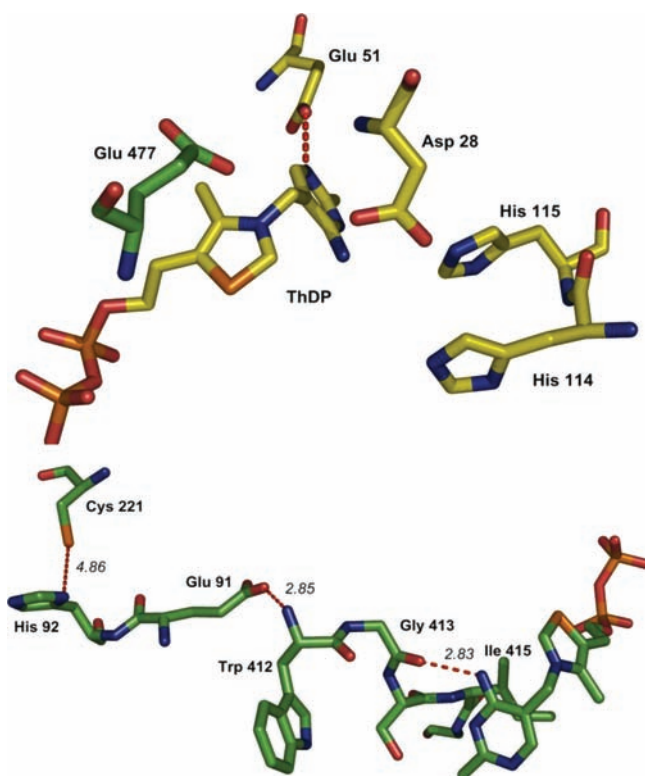


**Figure 1.** ThDP bound in the V confirmation at the active site of YPDC. (Top) Side chains of residues which potentially participate in proton transfer steps (Glu51, Glu477, Asp28, His114, and His 115) are shown. (Bottom) Connectivity between Cys221 at the regulatory site and the ThDP binding loop (410–415) via His92, Glu91, and backbone N and O atoms of Trp412 and Gly413. Coordinates were taken from the PVD1.pdb file and illustrated using Pymol.

information from pyruvate bound at C221) and thence the  $\gamma$  domain and the residues in a loop (residues 410–415) directly involved in ThDP binding<sup>28–31</sup>] were studied. To date, much of the information available on these YPDC variants is from steady state Michaelis–Menten kinetics and chemical quench NMR studies. Recently, phosphinate analogs of pyruvate and the most potent inhibitors of the pyruvate dependent E1 component of pyruvate dehydrogenase complexes.<sup>32</sup> In conjunction with CD experiments, detailed insights into the tautomeric states of intermediate analogs bound to YPDC under steady-state conditions and the rates of formation of such intermediates under presteady state conditions were obtained.<sup>10,33,34</sup>

In this report, we use multiple strategies to gain further insight to catalysis by YPDC by interrogating key active center acid–base groups: CD to monitor accumulation of a stable LThDP intermediate analog and pyruvate-derived intermediates, and rapid quench NMR to assess rate-limiting steps with these variants. The combination of these strategies allowed direct detection of the covalent intermediates (via NMR) and the tautomeric state of the accompanying 4'-aminopyrimidine ring (via CD). Since the current methods allow us to study the events in the active sites containing ThDP, effect of these substitutions on individual catalytic steps could be determined and the role of these residues in YPDC catalysis could be assessed with greater certainty.

## EXPERIMENTAL PROCEDURES

**Materials.** Alcohol dehydrogenase from yeast (ADH),  $\beta$ -mercaptoethanol (BME),  $\beta$ -NADH,  $\text{Na}_2\text{EDTA}$ , potassium phosphate, sodium pyruvate, morpholinoethanesulfonic acid (MES), phenylmethanesulfonyl fluoride (PMSF), thiamin hydrochloride, and thiamin diphosphate were obtained from Sigma Chemical Company (St. Louis, MO). Dithiothreitol (DTT) and isopropyl- $\beta$ -D-1-thiogalactopyranoside (IPTG) were from USB (Cleveland, OH).

Preparation of YPDC variants is described in the Supporting Information.

Synthesis of sodium propionylphosphinate (PP) was recently published.<sup>35</sup>

**Enzyme Purification.** All variants were overexpressed in *E. coli* BL21(DE3) strain. YPDC, E91D, E51D, E51N, E51A, and E477Q variants have a C-terminal His<sub>6</sub>-tag and were purified using a  $\text{Ni}^{2+}$  Sepharose column.<sup>22,24</sup> The E51Q, D28A, D28N, and C221E variants that have no His<sub>6</sub>-tag were purified as described elsewhere.<sup>22,36</sup> Protein concentration was determined by the Bradford method.<sup>37</sup>

**YPDC Assays.** Conversion of acetaldehyde to ethanol by yeast alcohol dehydrogenase in the presence of NADH was coupled to YPDC catalyzed production of acetaldehyde from sodium pyruvate. The disappearance of NADH is monitored at 340 nm using a Varian DMS 300 spectrophotometer.<sup>38</sup> The activity was measured in the presence of 20 mM pyruvate in standard assay buffer (50 mM MES, 1 mM ThDP, 2 mM  $\text{MgCl}_2$ , 0.2 mg/mL NADH, 0.08 mg/mL ADH, pH 6.0) at 30 °C. The reaction was started with addition of 3  $\mu\text{g}/\text{mL}$  YPDC. For the variants, higher concentrations of enzyme were used.

### Fluorescence Spectroscopy to Determine Binding of ThDP and N1'-methylThDP to YPDC and E51A YPDC.

The apo-E51A (3.0 mL, final concentration = 0.1 mg/mL) was first incubated with 0.003 mL  $\text{Mg}^{2+}$  (final concentration of 1 mM) and 2.697 mL of 100 mM MES, pH 6.0. Then aliquots of ThDP or N1'-methylThDP (NMThDP) were added and emission spectra were recorded from 300–450 nm. The experimental data were computer-fitted to the following equation:<sup>39</sup>

$$(\Delta F/F_0 \times 100) = \frac{(\Delta F_{\text{max}}/F_0 \times 100)[S]}{K_d + [S]} \quad (1)$$

where  $(\Delta F/F_0 \times 100)$  is the percent quenching (percent change in fluorescence relative to the initial value) following addition of ThDP or NMThDP at a concentration  $[S]$ , and  $K_d$  is the dissociation constant. Fitting was carried out using nonlinear regression with the Marquardt–Levenberg algorithm (SigmaPlot, Jandel Scientific), providing values of  $K_d$  and  $(\Delta F/F_0 \times 100)$ .

**Circular Dichroism Spectroscopy.** All CD spectra were recorded on a Chirascan CD Spectrometer from Applied Photophysics (U.K.) in a 1 cm path length cell in the near-UV (280–400) wavelength region.

**Titration Experiments with Propionylphosphinate (PP).** To 2.4 mL of YPDC or its variants in 20 mM MES (pH 6.0) containing 0.5 mM ThDP and 2.5 mM  $\text{MgCl}_2$  was added an aliquot of PP from a 1 M stock solution to achieve the desired concentration. The mixture was allowed to equilibrate for 1 min and the CD spectrum was recorded at 25 °C. The titration was performed over a PP concentration range of 0.5–40 mM. For quantitative analysis, the CD signal intensity of the IP (positive near 300 nm) and Michaelis complex (negative

near 330 nm) bands corrected for dilution was plotted against PP concentration. Apparent dissociation constants ( $K_d^{app}$ ) were calculated by fitting the data to a Hill function described in eq 2 using SigmaPlot v.7.0.

$$CD_{297} = CD_0 + \frac{CD_{297}^{max} [PP]^{n_H}}{(K_d^{app})^{n_H} + [PP]^{n_H}} \quad (2)$$

In this expression  $CD_{297}$  is the observed CD signal at the given wavelength,  $CD_0$  the CD signal of the protein at this wavelength in the absence of PP,  $CD_{297}^{max}$  the maximum CD signal at saturation with PP,  $[PP]$  the concentration of substrate analog, and  $n_H$  the Hill coefficient.

**Titration Experiments with Pyruvate.** Experiments were performed with low activity variants and at 5 °C to slow down side reactions leading to carbonylase products. To 2.4 mL of YPDC variants (2.75 mg/mL) at 5 °C in 20 mM MES (pH 6.0) containing 0.5 mM ThDP and 2.5 mM  $MgCl_2$ , an aliquot of pyruvate from a 1 M stock solution was added to achieve the desired concentration. The mixture was stirred for 30 s and the CD spectrum was recorded at 5 °C. Additional aliquots of pyruvate were added until no further changes in CD spectra were observed.

**Stopped-Flow CD Spectroscopy (SF-CD).** Kinetic traces were recorded on a Pi\*-180 stopped-flow CD spectrometer (Applied Photophysics, U.K.) using 10 mm path length at the specified wavelengths. Data were recorded at 302 nm for PP and at 313 nm for pyruvate experiments. Temperature was maintained at 10 °C for YPDC with pyruvate, and at 30 °C for YPDC variants with pyruvate experiments.

**Presteady State Formation of 1',4'-Iminopyrimidine Tautomer of C2-(1-phosphino-1-propanol)ThDP.** A solution of YPDC (8 mg/mL) in 20 mM MES (pH 6.0) containing 0.5 mM ThDP and 2.5 mM  $MgCl_2$  in one syringe was mixed rapidly with an equal volume of PP (40 mM) in the same buffer placed in the second syringe. A total of 20 000 data points were recorded over a period of 90 s. Data from six repetitive shots were averaged and the raw data were smoothed using the Savitsky-Golay function provided by the accompanying software and fit to a single-exponential model as in eq 3 using SigmaPlot v.7.0.

$$CD_{302}(t) = CD_1 e^{-k_1 t} + c \quad (3)$$

**Presteady State Formation of 1',4'-iminolThDP and 1',4'-iminoHThDP.** A solution of YPDC (8 mg/mL) or variants in 20 mM MES (pH 6.0) containing 0.5 mM ThDP and 2.5 mM  $MgCl_2$  in one syringe was mixed rapidly with an equal volume of pyruvate (40 mM) in the same buffer placed in the second syringe. 20,000 data points (2000 for YPDC) were recorded over a period of 2, 20, and 50 s for YPDC, E51D, and E477Q variants, respectively. Data from ten repetitive shots were averaged and fit to a double-exponential model as in eq 4 using SigmaPlot v.7.0.

$$CD_{313}(t) = CD_1 e^{-k_1 t} + CD_2 e^{-k_2 t} + c \quad (4)$$

**<sup>1</sup>H NMR Spectroscopy for Detection of ThDP-Bound Intermediates.** NMR spectra were acquired on a Varian 600 MHz instrument. The water signal was suppressed by presaturation. 4096 scans were collected with a recycle delay of 2.5 s, 32 000 data points per scan, and 12 ppm spectral width.

**Steady-State Distribution of Covalent ThDP Intermediates in Glu51 Variants.** 200  $\mu$ L of E51 YPDC variants (E51D: 5 mg/mL; E51Q: 15 mg/mL; E51A: 24 mg/mL) in 20 mM MES (pH 6.0) was mixed with 200  $\mu$ L of pyruvate (0.1 M) in the same buffer. In the case of variant E51A, the buffer additionally contained 1 mM ThDP and 5 mM  $MgCl_2$ . The reaction was incubated at 25 °C for defined times assuring establishment of the true steady state (E51D and E51Q: 30 s, E51A: 180 s) and quenched with 200  $\mu$ L of 12.5% TCA in 1 M DCl/D<sub>2</sub>O. The mixture was centrifuged at 14,000 rpm for 30 min and the supernatant was filtered through a Gelman Nylon Acrodisc (0.45  $\mu$ m). The filtrate was used for <sup>1</sup>H NMR analysis as reported initially by Tittmann et al.<sup>16</sup> and on YPDC 291–300 loop variants by Joseph et al.<sup>40</sup> ThDP and ThDP-bound intermediates are stable under the acid quench conditions of the experiments (pH 0.75). The <sup>1</sup>H chemical shift of the C6'-H resonances differ in various ThDP-bound intermediates and thus in a reaction mixture can be identified unambiguously, while their relative integrals provide a quantitative estimate of the relative abundance of the intermediates.

**Transient State Distribution of Covalent ThDP Intermediates in E51 Variants.** 200  $\mu$ L of E51 YPDC variants (E51D: 5 mg/mL; E51A: 24 mg/mL) in 20 mM MES (pH 6.0) was mixed with 200  $\mu$ L of pyruvate (0.1 M) in the same buffer. In case of variant E51A, the buffer additionally contained 1 mM ThDP and 5 mM  $MgCl_2$ . Reaction was allowed to proceed for either 35 ms (E51D) or 2 s (E51A) and was then quenched with 200  $\mu$ L of 12.5% TCA in 1 M DCl/D<sub>2</sub>O using a rapid quench instrument (RQF-3 from KinTek). Sample workup and NMR spectroscopic analysis was carried out as detailed in the previous paragraph (RCQ-NMR).<sup>16,40</sup>

**Distribution of Covalent ThDP Intermediates in Slow Variants at 5 °C with Low Pyruvate Concentration.** 400  $\mu$ L of E477Q YPDC or E51D YPDC (25 mg/mL) in 20 mM MES (pH 6.0) containing 1 mM ThDP and 5 mM  $MgCl_2$  was mixed with 50  $\mu$ L of pyruvate (0.1 M). The reaction was incubated at 5 °C for 180 s and quenched with 200  $\mu$ L of 12.5% TCA in 1 M DCl/D<sub>2</sub>O. Sample workup and NMR spectroscopic analysis was carried out as detailed in the previous paragraph.<sup>16,40</sup>

## RESULTS

### Steady State Kinetic Studies of E51 YPDC Variants.

Due to the pronounced substrate-activation observed in the steady-state kinetics of YPDC, the data are discussed in terms of  $S_{0.5}$ , rather than  $K_M$ , as well as  $k_{cat}/S_{0.5}$  (rather than  $k_{cat}/K_M$ ) for the composite second order rate constant starting with addition of the first pyruvate to YPDC and culminating in the first irreversible step, decarboxylation of LThDP. The kinetic parameters for YPDC and the E51 variants (as well as for D28A, E477Q, C221E/C222A, and E91D, other variants used in this study) are summarized in Table 1 (pH dependent kinetic data are presented in Figures S1 and S2 in Supporting Information). Substitutions at this position elicited decreases in  $k_{cat}$  from 1000-fold for E51D substitution to 10 000-fold for E51A and E51N substitutions as compared to the YPDC. Both the negative charge and the distance between the side chain of residue 51 and the N1' atom of ThDP are important for catalytic activity. E51D, E51Q and E51N are still capable of forming a hydrogen bond with ThDP, albeit weaker, whereas H-bond formation is excluded in the E51A variant. The  $S_{0.5}$  values also increase by an order of magnitude and a maximal value of 31 mM is observed for the E51N variant compared to

**Table 1. Kinetic Parameters for YPDC and Its Variants Used in This Study**

variant	$k_{\text{cat}}$ ( $\text{s}^{-1}$ )/ <sup>a</sup> subunit	$n_{\text{H}}$	$S_{0.5}$ (mM)
YPDC	60	$1.88 \pm 0.06$	$1.1 \pm 0.2$
E51D	0.049	$1.39 \pm 0.05$	$23.1 \pm 1.3$
E51Q	0.035	$1.07 \pm 0.08$	$14.9 \pm 1.3$
E51N	0.0024	$1.34 \pm 0.2$	$31.5 \pm 12$
E51A	0.0043	$1.58 \pm 0.2$	$0.72 \pm 0.1$
D28A	0.066	$2.01 \pm 0.16$	$1.66 \pm 0.25^b$
E477Q	0.086	$1.49 \pm 0.11$	$3.02 \pm 0.22^b$
E91D	11	$1.86 \pm 0.14$	$1.79 \pm 0.22^c$
C221E/C222A	18.2	$1.05 \pm 0.02$	$1.47 \pm 0.04^d$

<sup>a</sup>Per subunit, there are four subunits. <sup>b</sup>From ref 22. <sup>c</sup>From ref 29. <sup>d</sup>From ref 43. This is a double mutant with a substitution at the neighboring Cys222 to eliminate potential complications. This substitution has no influence on the activity.

1.1 mM for YPDC, indicating that most substitutions at this position adversely affect substrate binding. The E51A variant displays anomalous behavior ( $S_{0.5} = 0.72$  mM), presumably reflecting the enlarged space. The one significant difference compared to an earlier report at this residue, is that in the current study, the E51A YPDC variant still retained nonzero residual activity.<sup>41</sup>

Results from chemical quench followed by <sup>1</sup>H NMR detection of ThDP-bound covalent intermediates reveal that the events at the active sites follow a similar trend with YPDC and E51D, showing significant occupancy of the active sites with intermediates, whereas the E51Q variant shows much lower level of occupancy and intermediates do not accumulate at detectable levels in the E51A variant (Figure 2). Clearly with the E51A variant, step(s) preceding addition of pyruvate to ThDP were rate limiting. Presumably, the activation of ThDP via formation of the APH<sup>+</sup> form is severely perturbed.

**Binding of ThDP and NMThDP to E51A YPDC. Is There a Binding Preference for the Charged APH<sup>+</sup> Species?** To test the role of the E51 residue in cofactor binding, and possible stabilization of the APH<sup>+</sup> form on YPDC, a fluorescence titration experiment was carried out by reconstitution of apo-E51A YPDC with ThDP and NMThDP. On addition of ThDP or NMThDP to apo-E51A YPDC in 100 mM MES (pH 6.0) quenching of intrinsic fluorescence (excitation at 290 nm, emission at 338 nm) is observed. The quenching of apo-E51A YPDC fluorescence by ThDP was concentration-dependent and displayed saturation of half of the active centers only, with  $K_d$  of 27  $\mu\text{M}$  (see Supporting Information, Figure S3). In contrast, binding of NMThDP displayed saturation of all sites with  $K_d = 5.4 \mu\text{M}$ . This experiment also suggests that the E51A substitution interrupts communication between active centers, resulting in saturation of only half of the sites by ThDP, such as was found with the corresponding E571A variant of *E. coli* pyruvate dehydrogenase E1.<sup>42</sup> Since the E51A has more space for the N1'-methyl group of the analog, the stronger binding of NMThDP than ThDP to this E51A variant is reasonable and clearly indicates that the 4'-aminopyrimidine ring contributes to binding. The experiments with NMThDP also imply that the 4'-aminopyrimidine-binding cleft is designed to stabilize the APH<sup>+</sup> form of ThDP electrostatically, as also found with the E571A variant of *E. coli* pyruvate dehydrogenase E1.<sup>42</sup> This is the form, which can partition to the three neutral forms, AP, IP and the ylide in Scheme 1. Importantly, since no CD signatures

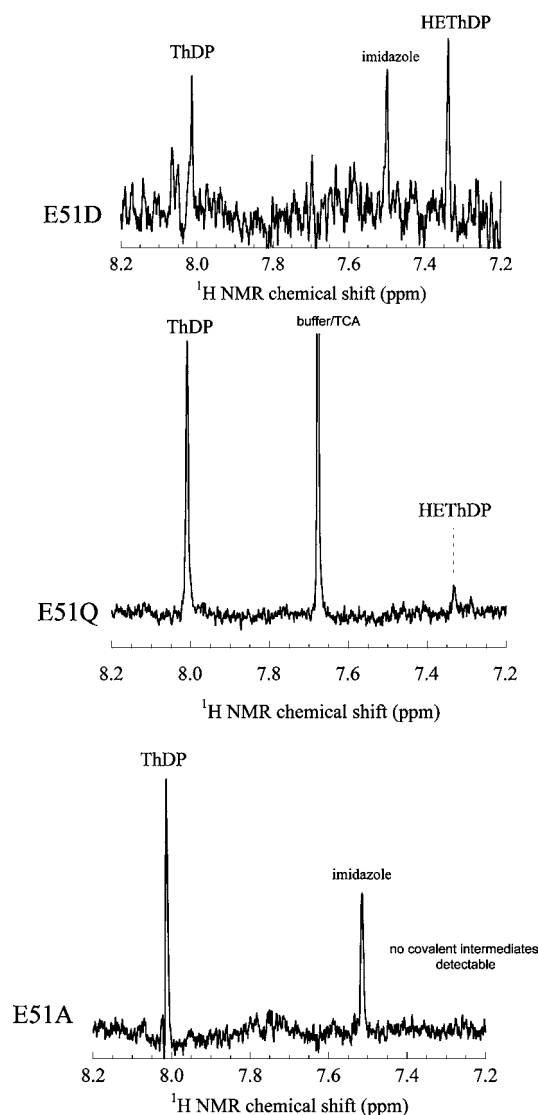


**Figure 2.** Distribution of ThDP covalent intermediates of Glu51 variants during steady state. C6'-H fingerprint region in <sup>1</sup>H NMR spectra acquired with after acid quench of the reaction of (top) E51D YPDC (5 mg/mL), (middle) E51Q (15 mg/mL), and (bottom) E51A (24 mg/mL) with 100 mM pyruvate. All spectra were acquired at 25 °C and pH 0.75. Acquisition parameters are described under Experimental Procedures.

are available for the APH<sup>+</sup> form, this experiment provides important support for the proposed notion.

**Tautomeric Forms of ThDP on YPDC Observed with PP Binding.** Upon titration of YPDC with PP, two CD bands developed simultaneously: (i) a positive band at 297 nm and (ii) a negative band at 330 nm (Figure 3, top). The spectra were reminiscent of an analogous experiment with acetylphosphate reported earlier.<sup>10</sup> The observed positive CD band at 297 nm could be assigned to the 1',4'-iminopyrimidine tautomer (IP form) of C2-(1-phosphino-1-propanol)ThDP (PPTHDP), and the negative CD band at 330 nm to a Michaelis complex consisting of enzyme, substrate analog and ThDP (Scheme 1B).<sup>10–15</sup> Simultaneous development of both bands suggested that the four active sites exist in two distinct tautomeric/ionization states in the presence of PP; that is, they are asymmetric. The titration data fit to the Hill equation revealed sigmoidal binding characteristics with Hill coefficients

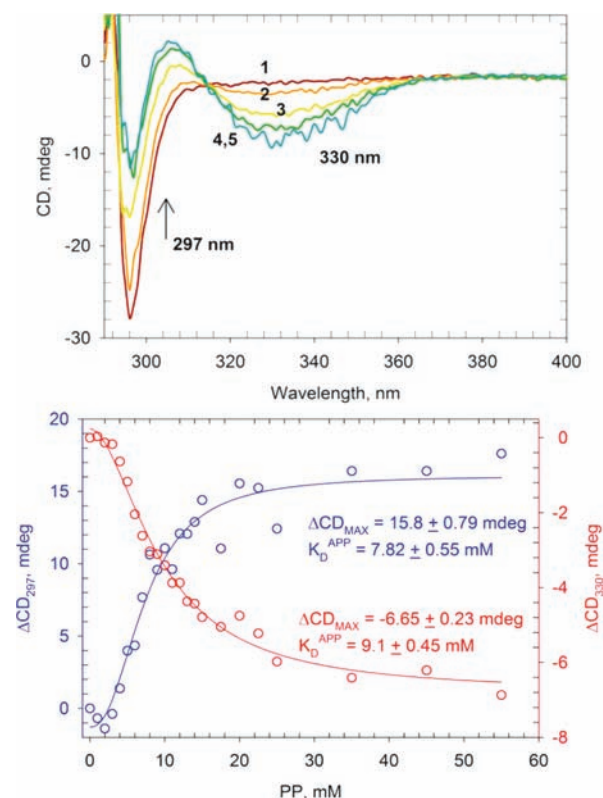


**Figure 3.** Formation of 1',4'-iminoPPTThDP on YPDC. (Top) Near UV (290–400 nm) CD spectra of YPDC (5.0 mg/mL) in absence of PP (1) and in presence of 5 mM PP (2), 10 mM PP (3), 20 mM PP (4), and 35 mM PP (5). The 1',4'-iminoPPTThDP species (Scheme 1B) is seen accumulating at 297 nm and the Michaelis complex (YPDC + PP) is seen accumulating at 330 nm. (Bottom) CD amplitude of IP form at 297 nm (blue circles) and of Michaelis complex at 330 nm (red circles) during titration plotted against concentration of PP.

of 2.63 for the IP form of PPTThDP and 2.13 for the Michaelis complex (Figure 3, bottom), suggesting that PP also binds at the regulatory sites and this binding event is recognized by the active sites. It is important to point out that the Michaelis complex is fully formed within the deadtime of the stopped flow instrument, while the rate of formation of the predecarboxylation intermediate or analog is on the stopped-flow time scale.

**Allosteric Activation Is Sensed by CD Spectroscopy at the Active Sites.** A CD titration of the E91D YPDC [the residue E91 is located on the  $\alpha$  domain at the intersection of the three domains on the information transfer pathway emanating from the  $\beta$  domain (C221) to the  $\gamma$  domain (binding ThDP)], with PP, once more displayed simultaneous formation of two bands (Figure 4, top). However, the data fit to the Hill equation revealed hyperbolic binding characteristics with a Hill coefficient of 1.08 for the IP form of PPTThDP and 1.5 for the Michaelis complex (Figure 4, middle). The  $K_D^{\text{APP}}$  values, estimate of affinity of active sites for PP, were similar for this variant and YPDC (Table 2). The data indicate that the E91D YPDC retains its affinity for PP at the asymmetric active sites notwithstanding disrupted communication with the regulatory site, as also seen earlier for pyruvate by Michaelis-Menten kinetics.<sup>29</sup>

In the C221E/C222A variant cysteine is replaced by glutamate, and this mimics pyruvate covalently bound to C221 in the hemithioacetal form, thus producing a permanently

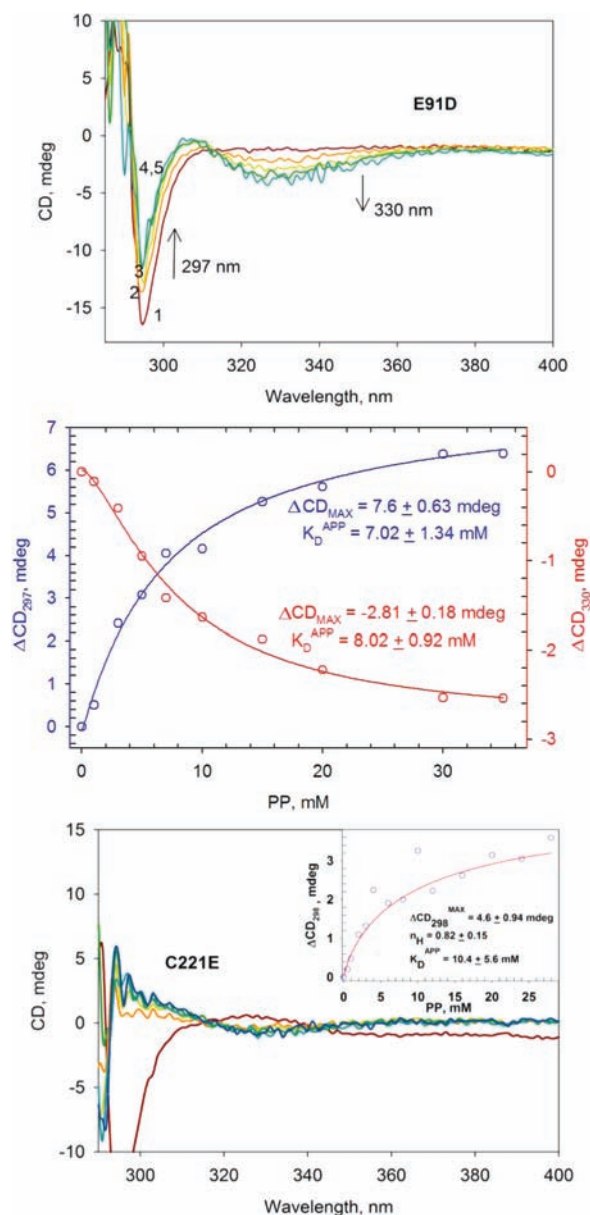


**Figure 4.** Formation of 1',4'-iminoPPTThDP on the E91D and C221E/C222A substrate activation pathway variants. (Top) Near UV (290–400 nm) CD spectra of titration of E91D YPDC (2.75 mg/mL) (1) and in presence of 5 mM PP (2), 10 mM PP (3), 20 mM PP (4) and 35 mM PP (5). The 1',4'-iminoPPTThDP species is seen accumulating at 297 nm and the Michaelis complex at 330 nm. (Middle) CD amplitude of IP form at 297 nm (blue circles) and of Michaelis complex at 330 nm (red circles) plotted against concentration of PP. The data points were fitted to the Hill equation and the regression fit lines are displayed. (Bottom) Near UV (290–400 nm) CD spectra of C221E/C222A YPDC (2.75 mg/mL) (brown). Difference spectra obtained after subtraction of spectrum in the absence of PP from those in presence of 1–28 mM of PP. The 1',4'-iminoPPTThDP species is seen accumulating at 298 nm. (Inset) Dependence of CD amplitude at 298 nm on PP concentration. The data points (circles) were fitted to a Hill equation and the regression fit line is displayed.

activated YPDC form. This variant showed only 2–5-fold reduction in activity compared to YPDC and hyperbolic Michaelis–Menten kinetics were observed.<sup>43</sup> In a CD titration experiment with PP, again both CD bands were observed but with reduced intensities (Figure 4, bottom). The titration data

**Table 2. Equilibrium Binding Parameters of PP to YPDC Variants from CD<sup>a</sup>**

variant	$K_d^{app}$ (mM)	Hill coefficient, $n_H$	CD max (mdeg)
	$9.1 \pm 0.45$ (MC)	$2.13 \pm 0.2$ (MC)	$-6.65 \pm 0.23$ (MC)
YPDC	$7.82 \pm 0.55$ (IP)	$2.63 \pm 0.45$ (IP)	$15.8 \pm 0.79$ (IP)
E91D	$8.02 \pm 0.92$ (MC)	$1.5 \pm 0.2$ (MC)	$-2.85 \pm 0.18$ (MC)
	$7.02 \pm 1.34$ (IP)	$1.1 \pm 0.16$ (IP)	$7.6 \pm 0.63$ (IP)
C221E	$7.83 \pm 3.48$ (IP)	$1.0 \pm 0.22$ (IP)	$4.7 \pm 0.77$ (IP)
E51D	$13.6 \pm 0.35$ (IP)	$2.7 \pm 0.2$ (IP)	$21.6 \pm 0.54$ (IP)
E477Q	not detected		
D28A	not detected		

<sup>a</sup>MC, Michaelis complex; IP, 1',4'-iminopyrimidine tautomer of PThDP.

fit to the Hill equation revealed hyperbolic binding characteristics with a Hill coefficient of 1.0 for the IP form. Since with this substitution, PP cannot bind at the regulatory site of the enzyme, allosteric activation is completely abolished.

**Active Center Substitutions Severely Impact PP Binding.** With the E51D substitution, addition of PP produces only the positive CD band at 297 nm (Figure 5, top) pertaining to the enzyme bound 1',4'-iminoPThDP intermediate, but gave no evidence of the negative CD band at 330 nm pertaining to the Michaelis complex. Titration data fit to the Hill equation revealed sigmoidal binding characteristics and a Hill coefficient of 2.74, similar to the value observed with YPDC. Allosteric regulation by PP is still seen in the formation of the tetrahedral intermediate analog. Apparently, the aspartate in E51D YPDC can still protonate the N1' atom, a necessary step enroute to formation of the first tetrahedral (predecarboxylation) adduct and stabilization of the IP tautomer, however the stabilization of the Michaelis complex observed in the presence of substrate analog in YPDC is disrupted in this variant.

The residue D28 ( $\alpha$  domain) and E477 ( $\gamma$  domain) are on different subunits and their substitutions disrupt the domain-domain (and subunit-subunit) interactions required for activity.<sup>7,8</sup> Upon titration of E477Q and D28A active-site variants with PP, only a weak positive CD band at 297 nm was observed in both cases (Figure 5 middle, bottom) but not the negative CD band at 330 nm. These active site substitutions severely affect (i) PP binding (Michaelis complex formation) and (ii) formation of 1',4'-iminoPThDP with PP. Residues D28 and E477 are situated above the thiazolium ring in position to interact with the pyruvate carboxylate group. Their substitutions apparently affect the binding of PP in a productive conformation, which in turn also affect addition of thiazolium C2 to the carbonyl group of PP.

**Tautomeric States of ThDP Observed during Catalytic Cycle of YPDC Variants with Pyruvate.** The low activity active center variants of YPDC (E51D, D28A, and E477Q) also accumulate intermediates under steady-state conditions and the rate of conversion between intermediates is slow. The tautomeric and ionization states of enzyme bound ThDP intermediates on the YPDC pathway could be determined using these variants. CD titration experiments were performed at 5 °C and pyruvate concentrations were in the range of 1–7 mM (typical  $S_{0.5}$  range for these variants), to minimize production of chiral acetoin and/or acetolactate via the carboligase side reactions.

Addition of 1 mM pyruvate to the E477Q YPDC produced two CD bands: (i) broad positive band with  $CD_{max}$  at 297 nm

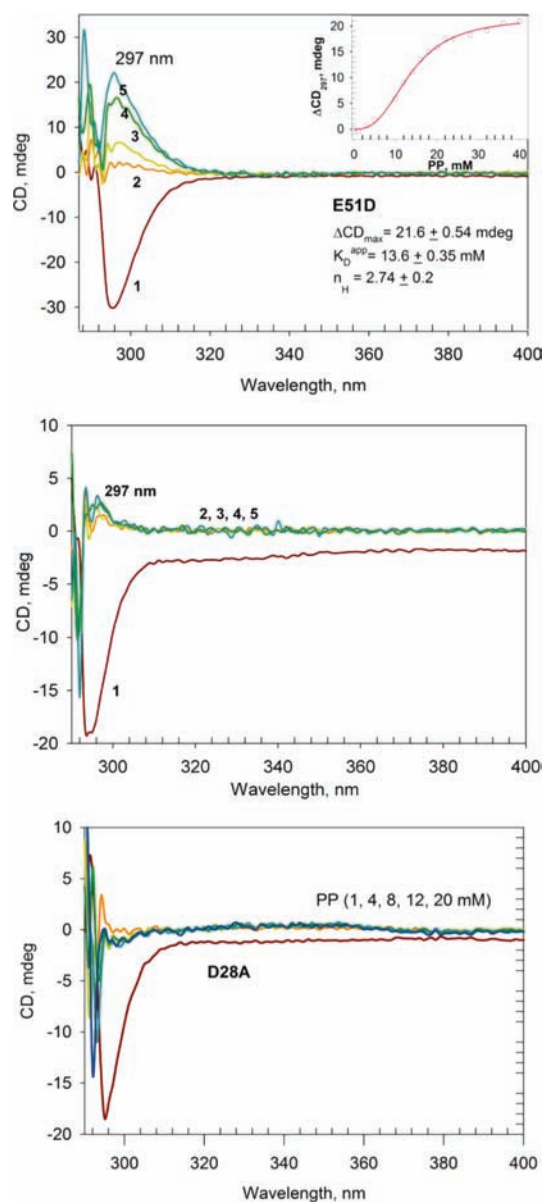


**Figure 5.** Formation of 1',4'-iminoPThDP on D28A, E51D, and E477Q active site variants. (Top) Near UV (290–400 nm) CD spectrum of E51D YPDC (5.0 mg/mL) (1). Difference spectra obtained after subtraction of (1) from spectra in the presence of 5 mM (2) 10 mM (3) 20 mM (4), and 40 mM (5) PP. The 1',4'-iminoPThDP species is seen accumulating at 297 nm. (Inset) Dependence of signal amplitude at 297 nm on PP concentration. The data points (circles) were fitted to a Hill equation and the regression fit line is displayed. (Middle) Near UV (290–400 nm) CD spectrum of E477Q YPDC (2.75 mg/mL) (1). Difference spectra obtained after subtraction of (1) from those in the presence of: 5 mM (2) 10 mM (3), 20 mM (4), and 40 mM (5) PP. The 1',4'-iminoPThDP species is seen accumulating at 297 nm. (Bottom) Near UV (290–400 nm) CD spectrum of D28A YPDC (2.75 mg/mL) (brown). Difference spectra obtained after in the presence 4–20 mM of PP.

for the IP form of a tetrahedral intermediate and (ii) broad negative band centered on 340 nm for the Michaelis complex (Figure 6, top). With further addition of pyruvate up to 5 mM, the bands showed negligible changes. The pyruvate induced active-site asymmetry observed in these spectra is similar to those observed on addition of PP in this work or

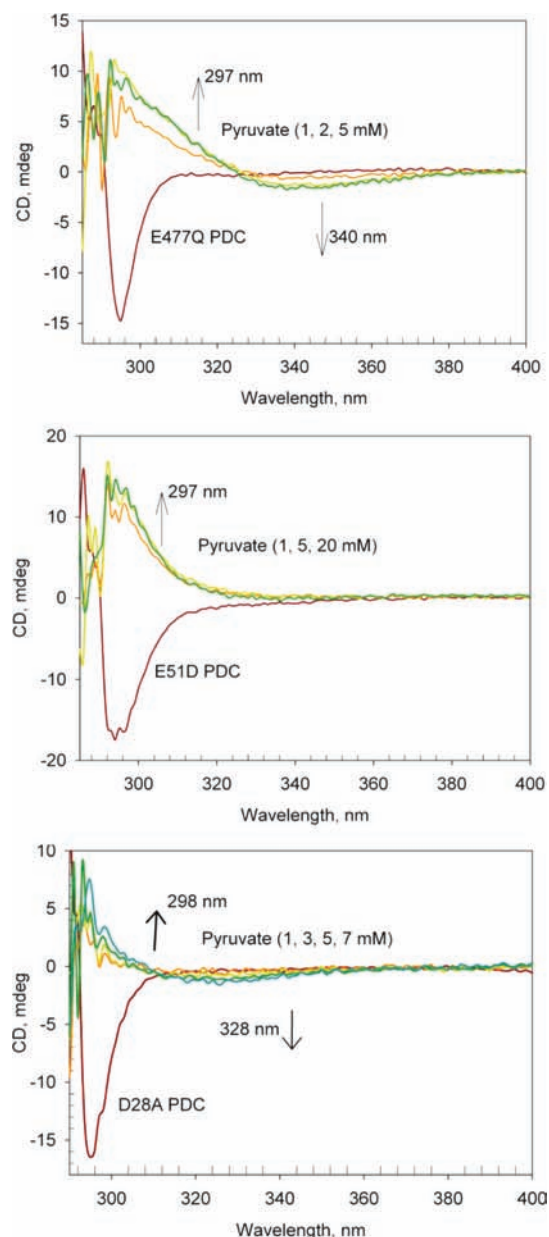


**Figure 6.** Formation of 1',4'-iminoLThDP and Michaelis complex on the D28A, E51D, and E477Q active site variants from pyruvate under steady state. Near UV (290–400 nm) CD spectra of (Top) E477Q YPDC (2.75 mg/mL) (brown) and difference spectra in the presence of pyruvate (1, 2, and 5 mM). (Middle) E51D YPDC (2.75 mg/mL) and difference spectra in the presence of pyruvate (1, 5, and 20 mM). (Bottom) D28A YPDC (2.75 mg/mL) (brown) and difference spectra in the presence of pyruvate (1, 3, 5, and 7 mM). In all cases the positive CD band with maxima at 297 nm pertains to the 1',4'-imino tautomer of a tetrahedral ThDP-bound intermediate, LThDP. The negative CD band centered at  $\sim 330$  nm pertains to the Michaelis complex and is absent in spectra of E51D YPDC.

acetylphosphinate to YPDC earlier.<sup>10</sup> This experiment confirms pyruvate-induced asymmetry of YPDC active sites.

Upon addition of 1 mM pyruvate to the E51D YPDC variant, similar to experiments with PP, a positive CD band with  $CD_{\max}$  at 297 nm was evident for IP form of LThDP, while the negative CD band at  $\sim 330$  nm was absent (Figure 6, middle). There was only a modest increase in amplitude upon further addition of 5 mM and even 20 mM pyruvate. Apparently, the

pyruvate-induced Michaelis complex formation is severely disrupted in this variant suggesting that the residue Glu51 has a role in stabilizing the Michaelis complex. This observation also provides a physical explanation for the observed increase in  $S_{0.5}$  for pyruvate for this variant (Table 1).

Neither CD band developed with significant amplitude on addition of 1 mM pyruvate to the D28A YPDC, and 7 mM pyruvate was needed to produce even weak bands: positive at 298 nm and negative at 328 nm (Figure 6, bottom). For this variant, the pyruvate-dependent acetaldehyde production plot exhibited remarkable characteristics: the rate of acetaldehyde production increases sharply and reaches a maximum at 2.5–3 mM pyruvate concentration, followed by a dramatic decrease, attributed to apparent substrate inhibition.<sup>25</sup> This variant produces acetolactate predominantly and C2- $\alpha$ -acetolactyl-ThDP (ALThDP) is the major intermediate under steady-state conditions, as determined by chemical quench/NMR previously.<sup>16</sup> To place these results into context, at low pyruvate concentrations, due to the low population of tetrahedral intermediates (alternatively, Michaelis complex and the enamine predominate), the CD band at 297 nm could not be observed. At high pyruvate concentrations ALThDP builds up (addition of enamine to a second molecule of pyruvate) reflected at 297 nm, the wavelength at which the ThDP-bound tetrahedral intermediates are seen in their IP form. While (S)-acetolactate, the predominant enantiomer produced by this variant shows a positive  $CD_{\max}$  at 300 nm, no time dependence could be observed in the signal shown in the figure during course of the experiment at low pyruvate concentrations, affirming that no product was being formed during the experiment. Upon overnight incubation of the reaction mixture at 4 °C with 20 mM pyruvate, chiral (S)-acetolactate accumulated according to the positive  $CD_{\max}$  at 300 nm.

**Time-Resolved Spectroscopic Studies on YPDC Variants. Transient State Kinetic Studies of the Formation of 1',4'-Iminopyrimidine Tautomer of ThDP-Bound Covalent Intermediates.** To determine kinetic competence of the covalent intermediate(s) in the IP tautomeric form observed earlier, rapid mixing experiments were performed. While the high turnover rate of YPDC precluded any steady-state CD experiments, presteady state experiments enabled detection of the IP tautomer at 313 nm upon mixing of YPDC with saturating concentrations of pyruvate (40 mM in syringe B). Time dependent accumulation of species with positive CD signal at 313 nm was observed and the process reached a steady state within 0.2 s with a rate constant of  $312 \text{ s}^{-1}$  (Figure 7, top). No time dependent changes could be observed for the Michaelis complex signal at 330 nm; presumably this intermediate accumulates within the 1.5 ms dead-time of the instrument, as observed earlier.<sup>44,50,53</sup> Under substrate saturating conditions, when the rate of formation of Michaelis complex is very fast, the apparent rate of formation of LThDP intermediate approximates to the net forward rate constant  $k'_2$  in Scheme 1A. This observed rate constant ( $312 \text{ s}^{-1}$ ) is in very good agreement with a previously determined  $k'_2$  of  $294 \pm 20 \text{ s}^{-1}$  for YPDC reaction with pyruvate.<sup>16</sup> This kinetic observation suggests that the IP tautomer being detected pertains to the LThDP tetrahedral intermediate. Further evidence obtained from NMR detection of intermediates at presteady state is presented below (Figure 8, bottom).

Transient state experiments performed with the E477Q and E51D active site variants (Figure 7, middle and bottom)

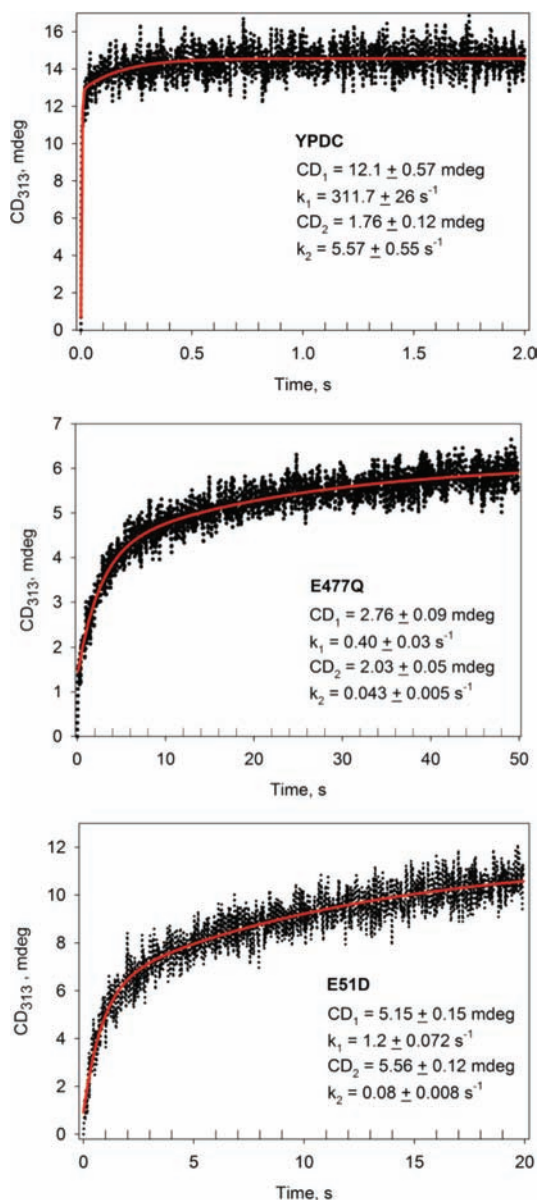


**Figure 7.** Time course of 1',4'-iminoLThDP formation in YPDC and the E51D and E477Q active site variants with pyruvate under presteady state conditions. Enzyme (8 mg/mL) was rapidly mixed with 40 mM pyruvate in a Pi<sup>\*</sup>-180 stopped-flow CD spectrometer and the CD signal was monitored at 313 nm. Data from 10 shots were averaged and the average was fitted to an exponential. The red trace for each spectrum is the regression fit line to double exponential. (Top) YPDC (8 mg/mL) for 2 s at 10 °C. (Middle) E477Q YPDC (8 mg/mL) for 50 s at 30 °C. (Bottom) E51D YPDC (8 mg/mL) for 20 s at 30 °C.

revealed similar time dependent accumulation of species with positive CD signals at 313 nm, with the processes following biphasic kinetics with rate constants of 0.4 and 0.04 s<sup>-1</sup> for E477Q, and 1.2 and 0.08 s<sup>-1</sup> for E51D. The rate constants are larger than the  $k_{cat}$  for these variants (Table 1) indicating that the intermediates detected are kinetically competent and transformation of these intermediates is probably among the rate limiting step(s). The biphasic kinetics observed most prominently in the case of E51D (both phases showing similar amplitudes of ~5 mdeg) also suggests the possibility of the

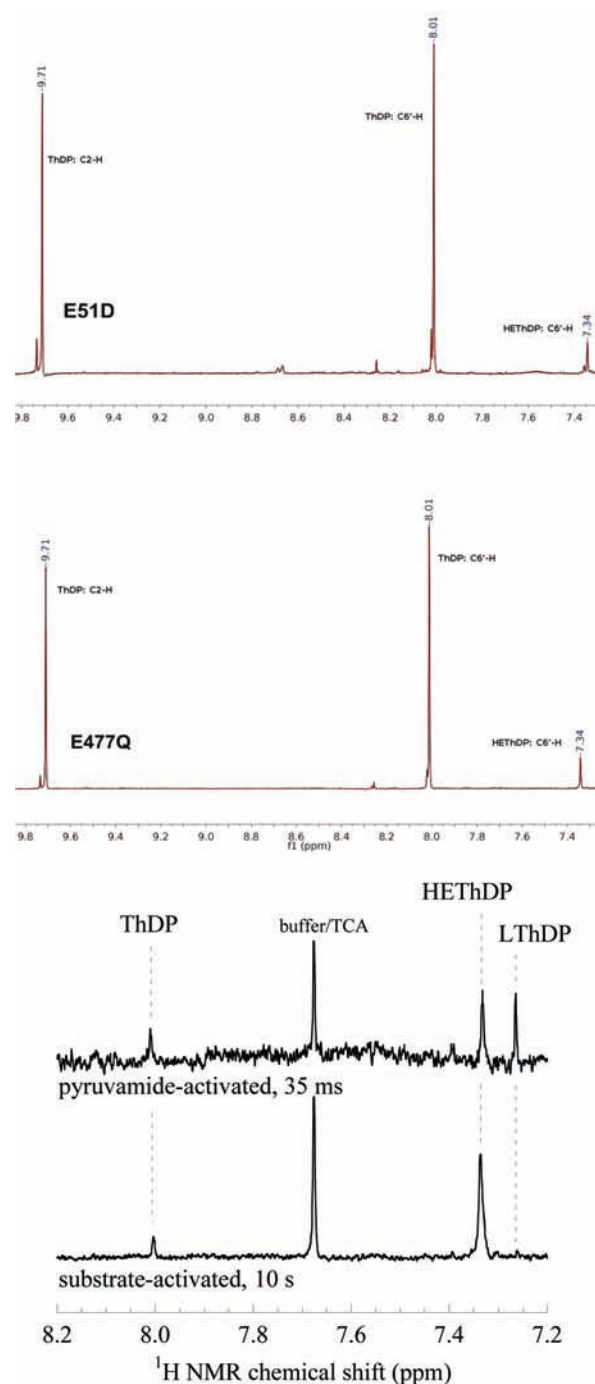


**Figure 8.** <sup>1</sup>H NMR detection of ThDP-bound intermediates under various conditions. Conditions of the steady-state CD titration experiment were replicated for the following: (Top) Reaction of E51D YPDC (25 mg/mL) with pyruvate (11 mM) at 5 °C was quenched with acid after 3 min. The supernatant containing the ThDP intermediates was analyzed by <sup>1</sup>H NMR using the characteristic C6'-H chemical shifts. [HETHDP]/[active sites] = 54.4% (determined from relative integrals of the corresponding signals after correction for excess ThDP from buffer). (Second from top) Reaction of E477Q YPDC (25 mg/mL) with pyruvate (11 mM) at 5 °C was quenched with acid after 3 min. [HETHDP]/[active sites] = 59%. (Bottom two) Distribution of covalent reaction intermediates in YPDC under steady state and transient state conditions. YPDC was either preincubated with activator pyruvamide (100 mM) for 10 min before mixing with substrate, or, alternatively, directly reacted with pyruvate as detailed in ref 16.

variants showing differing kinetic competencies at differing time-scales.

The above observations of the kinetic fate of the IP tautomer were next tested by identification of the ThDP-bound covalent intermediates accompanying the IP tautomer by chemical quench coupled to NMR identification during both transient and steady state time-scales.

**Chemical Quench/NMR Identification of ThDP-Bound Covalent Intermediates.**  $^1\text{H}$  NMR spectra of samples of E51D YPDC and E477Q YPDC prepared under steady-state reaction conditions as described under Experimental Procedures revealed the presence of HEThDP and LThDP in the active sites (Figures 2, 8, and 9). Relative integration of the C6'-

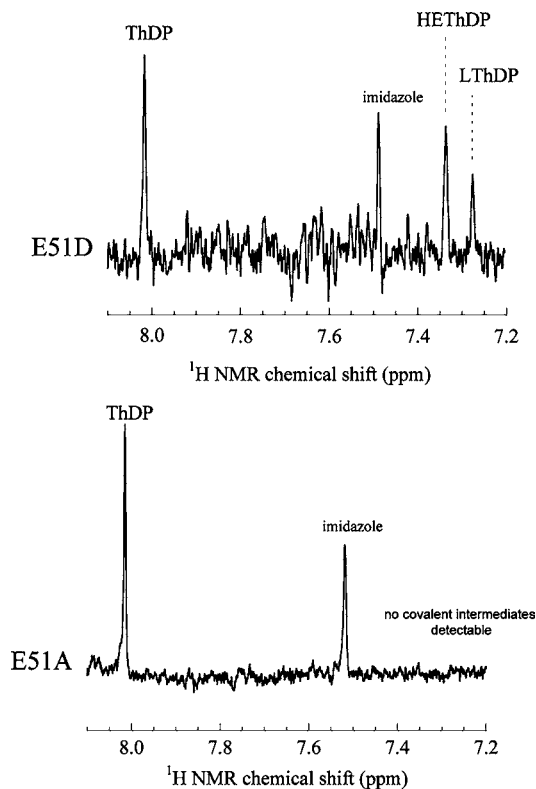


**Figure 9.** Distribution of ThDP-bound intermediates during transient state of Glu51 variants. C6'-H fingerprint region in  $^1\text{H}$  NMR spectra acquired with samples after acid quench of the reaction of (top) E51D YPDC (5 mg/mL) at 0.035 s and (bottom) E51A (24 mg/mL) at 2 s with 100 mM pyruvate. All spectra were acquired at 25 °C and pH 0.75. Acquisition parameters are described under Experimental Procedures.

H signals indicated that the active sites were filled with  $\sim 50\%$  by HEThDP in both variants (Figures 2, and Figure 8, top). HEThDP occupies most of the active sites during the steady state of YPDC with pyruvate.<sup>16</sup> Earlier reports showed that D28A YPDC in its reaction with pyruvate predominantly accumulates C2- $\alpha$ -acetolactylThDP, an intermediate also characterized on acetohydroxyacid synthase, and the E636Q variant of the *E. coli* pyruvate dehydrogenase E1 component.<sup>45,46</sup> These results allow straightforward assignments of CD observations as follows: (i) in E477Q YPDC, HEThDP in the IP form ( $\sim 50\%$ ) and Michaelis complex ( $\sim 50\%$ ); (ii) in E51D YPDC, HEThDP in the IP form ( $\sim 50\%$ ); and (iii) in D28A YPDC, C2- $\alpha$ -acetolactylThDP in the IP form ( $\sim 70\%$ ) and  $\sim 10\text{--}15\%$  Michaelis complex.

A transient state sample prepared by quenching the YPDC-pyruvate reaction at 35 ms showed the presence of LThDP, HEThDP and ThDP (Figure 8, bottom two). The fraction of covalent intermediates is larger, indicating that under presteady state conditions most of the active sites contain covalent intermediates. Transient state samples prepared by quenching the E51D YPDC-pyruvate reaction showed the presence of LThDP, HEThDP, and ThDP (Figure 9 top). The total occupancy of the covalent intermediates was  $\sim 50\%$  (LThDP + HEThDP), indicating that under presteady state conditions half the active sites are occupied with varying covalent intermediates while the other half are possibly unoccupied (i.e., no Michaelis complex). In conjunction with the transient state kinetics, these results indicate that on YPDC the LThDP accumulates in its IP form at the measured rate constant of  $311\text{ s}^{-1}$  during the transient state, while during the steady state the rate of decarboxylation of the accumulated LThDP becomes greater than its formation and thus only HEThDP/enamine accumulates. This analysis is extended also to transient state experiments on E51D YPDC, where both LThDP and HEThDP are detected by NMR analysis during presteady state (Figure 9) and HEThDP is detected during steady state (Figure 2). In this case LThDP accumulates in its IP form with a rate constant of  $1.2\text{ s}^{-1}$ .

Interestingly, substitution of the conserved Glu51 residue does not affect accumulation of the IP tautomer in contrast to accumulation of the Michaelis complex (also note increased  $S_{0.5}$  pyruvate and  $K_d^{\text{PP}}$  for PP). The environment around N1' still favors protonation but at a slower rate compared to YPDC. However, abolishing the acid residue as in E51A, produced a variant, which does not accumulate covalent intermediates at levels detectable by  $^1\text{H}$  NMR (Figures 2 and 9). In this case, the N1' protonation step is severely compromised thus slowing down ylide formation.

## DISCUSSION

**Homotropic Allosteric Regulation and Co-operativity in YPDC.** Compared to the other well-studied ThDP-dependent decarboxylase from *Zymomonas mobilis* (ZmPDC), the YPDC has an added complication arising from substrate activation.<sup>1,26–31,40,47</sup> The Rutgers group has participated in the determination of the X-ray structure of YPDC and in the elucidation of the substrate activation pathway. The cumulative evidence on the latter issue mapped the activation pathway to Cys221 on the  $\beta$  domain of the enzyme, to which the substrate could bind in a thiohemiacetal form, bridging to His92 then onto E91 (both on the  $\alpha$  domain), thence to Trp412 of the ThDP binding loop on the  $\gamma$  domain (410–415) which also includes G413,<sup>28,29,31</sup> the latter being hydrogen bonded to the 4'-amino group of ThDP, a group we have shown is involved in acid–base chemistry on the enzyme (Figure 1, bottom).<sup>10–15</sup>

While X-ray structures provided direct evidence for large scale rearrangements in the quaternary and tertiary structures of activated YPDC and related nonoxidative decarboxylases,<sup>30,48,49</sup> the current study probes the effect of these changes in the individual active-sites. Substitutions at C221 and E91 produced variants, which showed similar behavior to YPDC with PP (Michaelis complex, PPTHDP and  $K_d^{\text{PP}}$ ) in CD experiments. However, with these substitutions, the binding curve was hyperbolic, indicating compromised communication between the allosteric and active sites (Table 2). These findings are similar to earlier results with Michaelis–Menten kinetics (Table 1), and in addition suggest that the allosteric regulation is

Table 3. Observation of ThDP Intermediates during Various Steps in Catalytic Cycle of YPDC

	thiazolium moiety	amino-pyrimidine moiety	conditions where observed	detection method	figure/ref
1	Michaelis complex	APH <sup>+</sup>	YPDC + PP; E477Q/D28A + pyruvate steady state	CD, SF-CD	Figures 3–5
2	LThDP	IP	YPDC + pyruvate transient state E51D + pyruvate transient state	SF-CD, RCQ-NMR	Figures 7–9
3	enamine	APH <sup>+</sup>	no direct detection with pyruvate		
4	HEThDP	IP	YPDC + pyruvate steady and transient states; E51D + pyruvate steady and transient states E477Q + pyruvate steady state	CD, SF-CD, NMR	Figures 2 and 6–9
5	ALThDP <sup>a</sup>	IP	D28A + pyruvate steady state	CD, NMR	Figure 6; ref 16

<sup>a</sup>C2- $\alpha$ -acetylThDP is an intermediate in acetolactate synthesis, which is a prominent side product of the D28A YPDC. It is not an intermediate in the YPDC catalytic cycle; however, it is relevant to the catalytic cycle of acetoxyacid synthase, a member of the ThDP superfamily.

achieved via control of individual steps starting with Michaelis complex formation.

While the substrate activation could be easily tested, the pathways involved in producing active site asymmetry are less clear. According to the “proton-wire mechanism” for communication between active sites initially proposed by Frank et al.,<sup>50</sup> and most recently experimentally supported on the E1 component of pyruvate dehydrogenase complex from *E. coli*,<sup>42</sup> a direct pathway connecting the N1' atoms of ThDP from two connected active-centers could be imagined for YPDC with the conserved Glu playing a prominent role. This would be different from the pathway suggested in ref 50 since the direct pathway between two E51 residues in a functional dimer also includes residues capable of hydrogen bonding, but not of proton shuttling (Supporting Information Figure S5). Replacing glutamate by aspartate in E51D variant produced CD spectra reminiscent of other ThDP enzymes with non-communicating active sites, i.e., no Michaelis complex was observed. However, the increased  $S_{0,5}$  for E51 variants and  $K_d^{PP}$  of PP for E51D suggest that the substitutions produce variants with reduced ability to stabilize the Michaelis complex.

**Michaelis Complex in YPDC Catalysis.** The Michaelis complex, observed as a negative CD band at 330 nm in the presence of pyruvate or PP, is the noncovalent enzyme substrate/substrate analog intermediate in YPDC catalysis (Scheme 1, parts A and B). The Michaelis complex is proposed to comprise the enzyme bound ThDP and a pyruvate molecule bound to the active-site as detected on variants of the E1p component of *E. coli* pyruvate dehydrogenase complex with low catalytic activity.<sup>44,50,53</sup> However, this intermediate does not accumulate upon titration of either parental E1p or pyruvate oxidase with PP (see the Supporting Information, Figure S4). The present study with YPDC variants provides some insight into the minimal conditions necessary for accumulation of the Michaelis complex at levels detectable by CD spectroscopy.

YPDC, its E91D and C221E variants stabilize the Michaelis complex in the presence of acetyl- phosphinate, methyl acetylphosphonate<sup>10,14</sup> and PP. However, substitutions at the active site perturb the stabilization of this intermediate. The residue Glu51 appears to be necessary for stabilization of the enzyme-ThDP-pyruvate or enzyme-ThDP-PP Michaelis complex. Considering the conserved role of this residue in protonation of the N1' position of the 4'-aminopyrimidine ring, it can be concluded that the APH<sup>+</sup> state of ThDP is an essential component of the Michaelis complex. The D28A and E477Q variants failed to accumulate the Michaelis complex upon titration with PP. These residues are positioned above the thiazolium ring closer to the pyruvate-binding site.

Perturbations at these positions possibly affect optimal binding of PP in the active site and thus preclude formation of the Michaelis complex. Together, these observations suggest that ThDP in its APH<sup>+</sup> state (its activated state on enzymes<sup>52</sup>) and substrate bound at the active sites, in an orientation probably guided by the residues E477 and D28, are required for detection of the Michaelis complex by CD.

With pyruvate however, the E477Q and D28A variants do accumulate the Michaelis complex to varying extents indicating that pyruvate binds to the active site in the near attack conformation in these variants albeit with perturbations. Approximately 50% of the active sites in E477Q YPDC and 10–15% active sites in D28A YPDC are in the Michaelis complex form in a reaction with pyruvate according to NMR analysis of steady-state intermediate distribution. Possibly, the fact that PP is one CH<sub>2</sub> group longer than pyruvate, and the additional space needed on replacement of the trigonal carboxylate by the tetrahedral phosphorus environment, account for the difference in the behavior of PP compared to pyruvate.

**1',4'-Iminopyrimidine Tautomer of ThDP in YPDC Catalysis.** The 1',4'-iminopyrimidine tautomeric form of ThDP has been shown to accompany tetrahedral predecarboxylation intermediate analogs in 10 different members of the ThDP superfamily of enzymes to date. Also, the 1',4'-iminopyrimidine tautomeric form of ThDP was previously shown to accumulate during HEThDP formation in the reversible reaction with acetaldehyde on YPDC.<sup>15</sup> The current study for the first time provides evidence for formation of such intermediate in the forward direction of catalysis with pyruvate. While the steady-state CD spectroscopy experiments pointed toward accumulation of 1',4'-imino-HEThDP in the E51D and E477Q variants, chemical quench/NMR analysis at various time scales afforded snapshots of tetrahedral intermediate distribution during both steady-state and presteady state phases. Rate constants for LThDP formation on YPDC from NMR analysis, and rate constant for formation of 1',4'-iminopyrimidylLThDP from transient state CD spectroscopy are in very good agreement within experimental error; during short time-scales the 1',4'-iminopyrimidylLThDP was detected and kinetically characterized in the forward reaction.

Evidence for active-site asymmetry in the presence of pyruvate was found from experiments with E477Q YPDC and D28A YPDC during steady state. The coexistence of both predecarboxylation and postdecarboxylation intermediates in YPDC active sites is in agreement with a previous prediction by a model for alternating sites mechanism of catalysis of YPDC.<sup>54</sup> Additionally, detection of the IP form of ThDP in the presence

of C2 $\alpha$ -acetolactylThDP in D28A YPDC active sites provides further support for the notion that all tetrahedral C2 $\alpha$ -substituted ThDP intermediates are in the IP form at pH values near and above the pK<sub>a</sub> of the APH<sup>+</sup> form. Direct observation of the APH<sup>+</sup> form on three ThDP enzymes was recently achieved by solid state NMR methods.<sup>52</sup>

## CONCLUSION

To conclude, a summary of findings of this report is presented in Table 3, which clearly demonstrates the strength of combining steady state and transient state CD and <sup>1</sup>H NMR methods to elucidate individual steps on the reaction pathway (Scheme 1). There is now the possibility to obtain an ever more detailed microscopic picture of the pathway and to assign function to key amino acid residues on other ThDP enzymes with greater certainty.

## ASSOCIATED CONTENT

### Supporting Information

Site-directed mutagenesis methods for creation of E51 variants. Experimental procedures for assays for pyruvate decarboxylase and related pH dependent kinetic measurements. Experimental procedures for preparation of apo YPDC and reconstitution with ThDP and NMThDP. Figures depicting pH dependence of log(*k*<sub>cat</sub>) and *S*<sub>0.5</sub> for YPDC E51 variants. Spectra of tryptophan fluorescence quenching upon titration of apo E51A YPDC with ThDP and NMThDP. CD spectra of *E. coli* pyruvate dehydrogenase E1 component titration with PP. This material is available free of charge via the Internet at <http://pubs.acs.org>.

## AUTHOR INFORMATION

### Corresponding Author

frjordan@rutgers.edu.

### Notes

The authors declare no competing financial interest.

## ACKNOWLEDGMENTS

This work was supported at Rutgers by NIH-GM-050380 (to F.J.) and in part by Grant 126FP/0705M from the Ministry of Education of Saxony-Anhalt (to K.T.).

## REFERENCES

- (1) Boiteux, A.; Hess, B. *FEBS Lett.* **1970**, *9*, 293.
- (2) Hubner, G.; Konig, S.; Schellenberger, A. *Biomed Biochim Acta* **1988**, *47*, 9.
- (3) Sergienko, E. A.; Jordan, F. *Biochemistry* **2002**, *41*, 6164.
- (4) Konig, S.; Svergun, D.; Koch, M. H.; Hubner, G.; Schellenberger, A. *Eur Biophys J* **1993**, *22*, 185.
- (5) Killenberg-Jabs, M.; Jabs, A.; Lilie, H.; Golbik, R.; Hubner, G. *Eur. J. Biochem.* **2001**, *268*, 1698.
- (6) Muller, Y. A.; Lindqvist, Y.; Furey, W.; Schulz, G. E.; Jordan, F.; Schneider, G. *Structure* **1993**, *1*, 95.
- (7) Dyda, F.; Furey, W.; Swaminathan, S.; Sax, M.; Farrenkopf, B.; Jordan, F. *Biochemistry* **1993**, *32*, 6165.
- (8) Arjunan, P.; Umland, T.; Dyda, F.; Swaminathan, S.; Furey, W.; Sax, M.; Farrenkopf, B.; Gao, Y.; Zhang, D.; Jordan, F. *J. Mol. Biol.* **1996**, *256*, 590.
- (9) Schellenberger, A. *Biochim. Biophys. Acta* **1998**, *1385*, 177.
- (10) Nemeria, N.; Chakraborty, S.; Baykal, A.; Korotchkina, L. G.; Patel, M. S.; Jordan, F. *Proc. Natl. Acad. Sci. U.S.A.* **2007**, *104*, 78.
- (11) Jordan, F.; Nemeria, N. S.; Zhang, S.; Yan, Y.; Arjunan, P.; Furey, W. *J. Am. Chem. Soc.* **2003**, *125*, 12732.
- (12) Baykal, A. T.; Kakalis, L.; Jordan, F. *Biochemistry* **2006**, *45*, 7522.

- (13) Jordan, F.; Zhang, Z.; Sergienko, E. *Bioorg. Chem.* **2002**, *30*, 188.
- (14) Nemeria, N.; Baykal, A.; Joseph, E.; Zhang, S.; Yan, Y.; Furey, W.; Jordan, F. *Biochemistry* **2004**, *43*, 6565.
- (15) Nemeria, N. S.; Chakraborty, S.; Balakrishnan, A.; Jordan, F. *FEBS J.* **2009**, *276*, 2432.
- (16) Tittmann, K.; Golbik, R.; Uhlemann, K.; Khailova, L.; Schneider, G.; Patel, M.; Jordan, F.; Chipman, D. M.; Duggleby, R. G.; Hubner, G. *Biochemistry* **2003**, *42*, 7885.
- (17) Brandt, G. S.; Nemeria, N.; Chakraborty, S.; McLeish, M. J.; Yep, A.; Kenyon, G. L.; Petsko, G. A.; Jordan, F.; Ringe, D. *Biochemistry* **2008**, *47*, 7734.
- (18) Maraite, A.; Schmidt, T.; Ansorge-Schumacher, M. B.; Brzozowski, A. M.; Grogan, G. *Acta Crystallogr. Sec. F Struct. Biol. Cryst. Commun.* **2007**, *63*, 546.
- (19) Mosbacher, T. G.; Mueller, M.; Schulz, G. E. *FEBS J.* **2005**, *272*, 6067.
- (20) Nemeria, N.; Korotchkina, L.; McLeish, M. J.; Kenyon, G. L.; Patel, M. S.; Jordan, F. *Biochemistry* **2007**, *46*, 10739.
- (21) Kaplun, A.; Binshtein, E.; Vyazmensky, M.; Steinmetz, A.; Barak, Z.; Chipman, D. M.; Tittmann, K.; Shaanan, B. *Nat. Chem. Biol.* **2008**, *4*, 113.
- (22) Liu, M.; Sergienko, E. A.; Guo, F.; Wang, J.; Tittmann, K.; Hubner, G.; Furey, W.; Jordan, F. *Biochemistry* **2001**, *40*, 7355.
- (23) Sergienko, E. A.; Jordan, F. *Biochemistry* **2001**, *40*, 7382.
- (24) Gao, Y. Ph.D. Dissertation, Rutgers University: Newark, NJ, 2000.
- (25) Sergienko, E. A.; Jordan, F. *Biochemistry* **2001**, *40*, 7369.
- (26) Baburina, I.; Dikdan, G.; Guo, F.; Tous, G. I.; Root, B.; Jordan, F. *Biochemistry* **1998**, *37*, 1245.
- (27) Baburina, I.; Gao, Y.; Hu, Z.; Jordan, F.; Hohmann, S.; Furey, W. *Biochemistry* **1994**, *33*, 5630.
- (28) Li, H.; Jordan, F. *Biochemistry* **1999**, *38*, 10004.
- (29) Li, H.; Furey, W.; Jordan, F. *Biochemistry* **1999**, *38*, 9992.
- (30) Jordan, F.; Nemeria, N.; Guo, F.; Baburina, I.; Gao, Y.; Kahyaoglu, A.; Li, H.; Wang, J.; Yi, J.; Guest, J. R.; Furey, W. *Biochim. Biophys. Acta* **1998**, *1385*, 287.
- (31) Baburina, I.; Li, H.; Bennion, B.; Furey, W.; Jordan, F. *Biochemistry* **1998**, *37*, 1235.
- (32) Nemeria, N. S.; Korotchkina, L. G.; Chakraborty, S.; Patel, M. S.; Jordan, F. *Bioorg. Chem.* **2006**, *34*, 362.
- (33) Meyer, D.; Neumann, P.; Parthier, C.; Friedemann, R.; Nemeria, N.; Jordan, F.; Tittmann, K. *Biochemistry* **2010**, *49*, 8197.
- (34) Chakraborty, S. Ph.D. Dissertation, Rutgers, the State University of New Jersey: Newark, NJ, 2006.
- (35) Shim, D. J.; Nemeria, N. S.; Balakrishnan, A.; Patel, H.; Song, J.; Wang, J.; Jordan, F.; Farinas, E. T. *Biochemistry* **2011**.
- (36) Wang, J.; Golbik, R.; Seliger, B.; Spinka, M.; Tittmann, K.; Hubner, G.; Jordan, F. *Biochemistry* **2001**, *40*, 1755.
- (37) Bradford, M. M. *Anal. Biochem.* **1976**, *72*, 248.
- (38) Holzer, H.; Schultz, G.; Villar-Palasi, C.; Juntgen-Sell, J. *Biochem. Z.* **1956**, *327*, 331.
- (39) Liu, R.; Sharom, F. J. *Biochemistry* **1996**, *35*, 11865.
- (40) Joseph, E.; Wei, W.; Tittmann, K.; Jordan, F. *Biochemistry* **2006**, *45*, 13517.
- (41) Killenberg-Jabs, M.; Konig, S.; Eberhardt, I.; Hohmann, S.; Hubner, G. *Biochemistry* **1997**, *36*, 1900.
- (42) Nemeria, N. S.; Arjunan, P.; Chandrasekhar, K.; Mossad, M.; Tittmann, K.; Furey, W.; Jordan, F. *J. Biol. Chem.* **2010**, *285*, 11197.
- (43) Wei, W.; Liu, M.; Jordan, F. *Biochemistry* **2002**, *41*, 451.
- (44) Kale, S.; Arjunan, P.; Furey, W.; Jordan, F. *J. Biol. Chem.* **2007**, *282*, 28106.
- (45) Tittmann, K.; Schroder, K.; Golbik, R.; McCourt, J.; Kaplun, A.; Duggleby, R. G.; Barak, Z.; Chipman, D. M.; Hubner, G. *Biochemistry* **2004**, *43*, 8652.
- (46) Nemeria, N.; Tittmann, K.; Joseph, E.; Zhou, L.; Vazquez-Coll, M. B.; Arjunan, P.; Hubner, G.; Furey, W.; Jordan, F. *J. Biol. Chem.* **2005**, *280*, 21473.
- (47) Hubner, G.; Weidhase, R.; Schellenberger, A. *Eur. J. Biochem.* **1978**, *92*, 175.

- (48) Kutter, S.; Weiss, M. S.; Wille, G.; Golbik, R.; Spinka, M.; Konig, S. *J. Biol. Chem.* **2009**, *284*, 12136.
- (49) Versees, W.; Spaepen, S.; Wood, M. D.; Leeper, F. J.; Vanderleyden, J.; Steyaert, J. *J. Biol. Chem.* **2007**, *282*, 35269.
- (50) Frank, R. A.; Titman, C. M.; Pratap, J. V.; Luisi, B. F.; Perham, R. N. *Science* **2004**, *306*, 872.
- (51) Jordan, F.; Arjunan, P.; Kale, S.; Nemeria, N. S.; Furey, W. J. *Mol. Catal. B Enzym.* **2009**, *61*, 14.
- (52) Balakrishnan, A.; Paramasivam, S.; Chakraborty, S.; Polenova, T.; Jordan, F. *J. Am. Chem. Soc.* **2012**, *134*, 665.
- (53) Kale, S.; Ulas, G.; Song, J.; Brudvig, G. W.; Furey, W.; Jordan, F. *Proc. Natl. Acad. Sci. U.S.A.* **2008**, *105*, 1158.
- (54) Sergienko, E. A.; Jordan, F. *Biochemistry* **2002**, *41*, 3952.